# Probabilistic fault displacement Hazard analysis in an extensional setting: Application to a strategic Dam and methodological implications

Alessio Testa, Paolo Boncio, Bruno Pace, Francesco Mirabella, Cristina Pauselli, Maurizio Ercoli, Eugenio Auciello, Francesco Visini, Stephane Baize

Engineering Geology 343 (2024) 107817

Contents lists available at ScienceDirect

Engineering Geology

journal homepage: www.elsevier.com/locate/enggeo

# Probabilistic fault displacement Hazard analysis in an extensional setting: Application to a strategic Dam and methodological implications

Alessio Testa [a,*], Paolo Boncio [a,b], Bruno Pace [a,b], Francesco Mirabella [c], Cristina Pauselli [c], Maurizio Ercoli [c], Eugenio Auciello [d], Francesco Visini [e], Stéphane Baize [f]

[a] INGEO Department, Università degli Studi G. d'Annunzio Chieti e Pescara, Via dei Vestini 31, 66100 Chieti, Italy
[b] UdA-TechLab Research Center, University "G. d'Annunzio" of Chieti-Pescara, Via dei Vestini 31, 66100 Chieti, Italy
[c] Dipartimento di Fisica e Geologia, Università di Perugia, Via Alessandro Pascoli, 06123 Perugia, Italy
[d] Dipartimento di Bioscienze e Territorio, Università degli studi del Molise, Contrada Fonte Lappone snc, 86090 Pesche, Italy
[e] Istituto di Geofisica e Vulcanologia, Via di Vigna Murata 605, 00143 Rome, Italy
[f] IRSN/PSP-ENV/SCAN/BERSSIN, Institut de Radioprotection et de Sûreté Nucléaire, Fontenay-Aux-Roses 92262, France.

ARTICLE INFO

*Keywords:*
Capable fault
Probabilistic Fault displacement hazard analysis
Earthquake geology
Normal fault
Northern Apennines

ABSTRACT

We present a Probabilistic Fault Displacement Hazard Analysis (PFDHA) for a strategic dam located in the Upper Tiber Valley (Northern Apennines of Italy) claimed to be sited on a supposed capable fault (Montedoglio fault). We verify the seismic capability of the Montedoglio fault through detailed geological and geophysical analyses. We find no evidence for considering the Montedoglio fault as an active and capable structure, the fault being constituted by a system of discontinuous parallel faults, apparently inactive since more than 56 ± 3 ka, and likely unable to nucleate strong surface rupturing earthquakes. Since the dam lies on the hanging wall of the closest major active fault of the area (Anghiari normal fault, ~1.5 km away), we investigate the likelihood of having distributed faulting at the dam's site in case of a strong surface-rupturing earthquake occurring on the Anghiari fault. We apply a probabilistic approach to obtain hazard curves of exceedance of vertical displacement at the dam's site for different rupture scenarios. We show that the mean hazard curve is always below an annual frequency of exceedance of $1 \times 10^{-5}$, corresponding to displacement values below 1 cm over 100,000 years of return period. The study highlights several weaknesses and uncertainties in using PFDHA with state-of-the-art models, suggesting the need for improvements to enhance their applicability in earthquake engineering geology practice.

## 1. Introduction

Earthquake surface faulting is the primary evidence of tectonic deformation resulting from coseismic slip along a fault plane (McCalpin, 2009). This might be the source of hazard (fault displacement hazard, FDH) for manmade structures, and might have a severe impact on the safety of critical facilities (power plants, dams) and networks (pipelines) and even urbanized and industrial areas (Youngs et al., 2003; Petersen et al., 2011; Cheng and Akkar, 2017; Yang and Mavroeidis, 2018; Di Naccio et al., 2020; Valentini et al., 2021; Iezzi et al., 2023; Hosseini and Rahimi, 2022; Melissianos et al., 2023).

In the literature, there are many examples of surface faulting earthquakes, the 6th February 2023 Turkey earthquake being the most emblematic example (Görüm et al., 2023). This specific earthquake-related hazard was initially investigated out in the assessment of nuclear power plants safety (Schlocker and Bonilla, 1963). Fault displacement hazard is currently getting increasing interest in earthquake engineering geology, even outside the nuclear industry development (e.g., Nemer, 2019). During the last decade in Italy, for instance, the potential for FDH at the site of an existing dam has recently become mandatory to be evaluated in national guidelines (Ministero delle Infrastrutture e dei Trasporti, 2019.; Basili et al., 2017; DMIT, 2014).

Surface faulting occurs along the trace of the principal fault, often accompanied by distributed ruptures. Following the original definition of Youngs et al. (2003), the principal fault is the surface along which seismic energy is released and is commonly identifiable as the fault segment which has released the greatest amount of offset. Principal faulting usually occurs along a single narrow trace or over a zone from a

* Corresponding author at: Via dei Vestini 31, 66100 Chieti, Italy.
*E-mail address:* alessio.testa@unich.it (A. Testa).

https://doi.org/10.1016/j.enggeo.2024.107817
Received 13 December 2023; Received in revised form 18 September 2024; Accepted 12 November 2024
Available online 16 November 2024

few to many meters wide. Distributed ruptures, also known as secondary ruptures, are those that occur on other faults, shears, or fractures off the principal fault. These secondary ruptures can occur on faults that are or are not structurally connected to the principal fault (Youngs et al., 2003; Baize et al., 2019; Nurminen et al., 2022). Avoidance strategies such as the "Alquist-Priolo Earthquake Fault Zoning Act" (Bryant and Hart, 2007), the planning guidelines used in New Zealand (Kerr et al., 2003) and the Italian guidelines for seismic microzonation (SM Working Group, 2015), represent mitigation strategies against FDH for land planning and the design of new buildings. For example, the width of the rupture zone is an important factor to account for when determining the safety distance for new infrastructures (Zhang et al., 2013). However, avoidance is not a suitable option for pre-existing facilities that cannot avoid crossing a capable fault, or in circumstances when the fault is discovered after building construction. In these cases, one possible strategy is to assess the likelihood of having a certain value of displacement at the facility using probabilistic methods based on empirical regressions, i.e., a Probabilistic Fault Displacement Hazard Analysis (PFDHA, Youngs et al., 2003). Then, based on the results from PFDHA, measures for compensating the hazard at the facility site can be evaluated. The PFDHA approach can assist risk-based decisions that consider the balance between safety and cost-effectiveness according to the performance-based engineering framework (Melissianos et al., 2023). For example, an engineering-based definition of a safety threshold of admissible displacement, for each infrastructure, could lead to specific risk mitigation strategies based on a numerical quantification of the hazard. The International Atomic Energy Agency (IAEA) recommends a PFDHA if a newly identified capable fault has the potential to affect an existing nuclear installation (International Atomic Energy Agency (IAEA), 2021; International Atomic Energy Agency (IAEA),

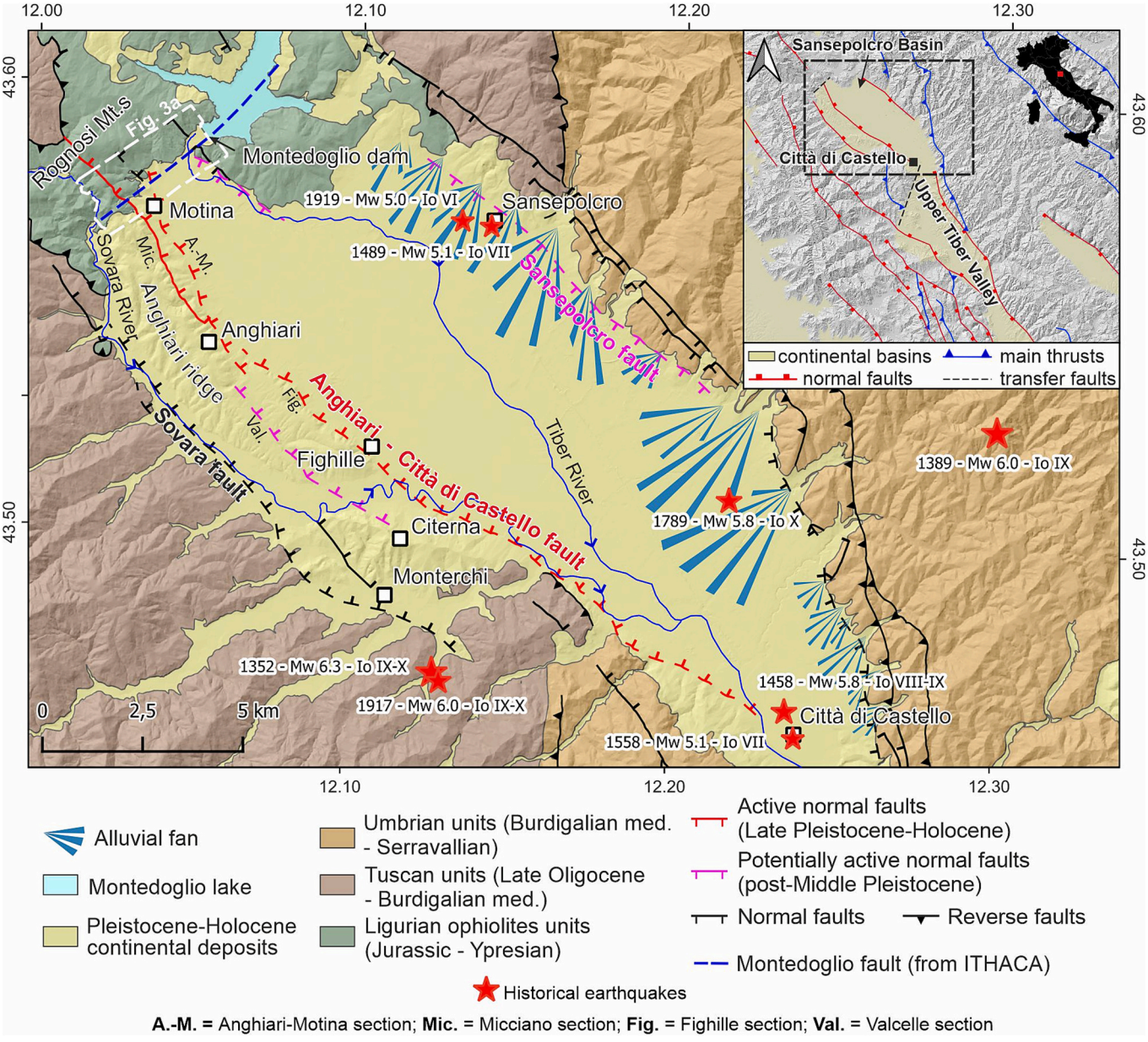


**Fig. 1.** Simplified geological map of the Sansepolcro basin showing the distribution of the main tectonic units, the continental deposits, the trace of the faults and the epicenters of historical earthquakes (red stars, the size of which scales with the magnitude; from Rovida et al., 2022). The faults affecting Upper Pleistocene-Holocene sediments are defined as active faults, while the faults affecting Middle Pleistocene deposits without further younger constraints are defined as potentially active. The white dashed box shows the location of Fig. 3. ITHACA = database ITaly HAzard from CApable faults (ITHACA Working Group: ITHACA (ITaly HAzard from CApable Faulting), 2019). (For interpretation of the references to colour in this figure legend, the reader is referred to the web version of this article.)

2022). IAEA defines a capable fault as a seismogenic fault with a significant potential for producing fault displacement at or near the ground surface, such as faults with evidence of significant deformation and/or dislocations of a recurring nature within such a period that it is reasonable to conclude that further movements at or near the surface may occur (International Atomic Energy Agency (IAEA), 2022). In highly seismically active areas International Atomic Energy Agency (IAEA) (2022) defines the Upper Pleistocene – Holocene as a reference period for evidence of past movements along the fault, while much longer periods (up to Pliocene) are recommended in less active areas (such as intraplate regions). Various methodologies of PFDHA, for evaluating both the hazard of principal and distributed faulting, have been proposed in the last 20 years for different faulting styles (Youngs et al., 2003; Petersen et al., 2011; Moss and Ross, 2011; Takao et al., 2013; Nurminen et al., 2020; Ferrario and Livio, 2021). Fault characterization through integration of structural, geophysical and paleoseismological investigation is crucial to get the fault parameters needed in PFDHA.

The focus of this study is PFDHA of the Montedoglio dam, built on the Tiber River in central Italy, at the northwestern edge of the Sansepolcro basin, in the Upper Tiber Valley (Fig. 1). The Montedoglio dam is a ≈ 60 m high and 570 m long earth-fill dam. It is a strategic facility (according to DMIT, 2014) as it is supplying 102 million cubic meters of potable water per year. According to the database ITHACA (ITaly HAzard from CApable faults, ITHACA Working Group: ITHACA (ITaly HAzard from CApable Faulting), 2019), this dam is crossed by a SW-NE striking oblique-slip capable fault (Montedoglio fault). Moreover, it is located close (~1.5 km) to the NE-dipping Anghiari normal fault which has been demonstrated to be capable by a previous paleoseismic study (Testa et al., 2023) and which is also included in ITHACA. The occurrence of a surface faulting earthquake along one of these two faults could pose a threat to the safety of the dam and, consequently, to the inhabitants of Upper Tiber Valley. For these reasons the Montedoglio dam is the target of our assessment of FDH considering both principal and distributed faulting hazards.

Although guidelines for evaluating FDH for existing dams in Italy are already available (Basili et al., 2017), specific instructions on how to conduct a FDH analysis are not given, and no published case studies are focused on this specific topic. The Italian guidelines for seismic microzonation (SM Working Group, 2015; Technical Commission on Seismic Microzonation, 2015), are designed for FDH of ordinary building and there are no references to strategic infrastructures.

This work presents the first case in Italy where a FDH study provides a quantitative probabilistic assessment of the expected displacement at the site of a dam.

We first address the activity and potential capability of the Montedoglio fault running beneath the dam, to assess principal faulting hazard: according to SM Working Group (2015), the fault would be considered capable if it shows evidence of surface displacement of a recurring nature in the last 40 ka based on detailed geological, geomorphological, geophysical and paleoseismological analyses. In addition, using the geometry and activity parameters of the Anghiari fault constrained by Testa et al. (2023), we assess the likelihood of having distributed faulting at the site of the dam by using the existing method of PFDHA for normal faulting proposed by Youngs et al. (2003). In a previous paper, Testa et al. (2021) tested this method, producing FDH maps for both principal and distributed faulting in the nearby Anghiari township. They highlighted the importance of constraining the principal fault, i.e., giving detailed fault location, slip rate, rupture scenarios and expected earthquake magnitude and surface displacement; they also highlighted the need to update the empirical regressions for distributed faulting. The normal faulting methodology of Youngs et al. (2003), uses regressions from 13 surface rupturing earthquakes of the Extensional Cordillera in western USA.

We used the Youngs et al.'s method as it is for both principal and distributed faulting, but we implemented the computation code with the new empirical regressions for distributed faulting obtained by Ferrario and Livio (2021), who updated empirical data for distributed ruptures until 2016. Moreover, we discuss limitations, uncertainties and methodological implications for future implementation of the PFDHA method, to improve its applicability in earthquake engineering geology practice.

## 2. Geological background

The northern Apennines are a NE-verging fold-and-thrust belt that deforms the Ligurian, Tuscan and Umbrian units (Pialli et al., 1998; Brozzetti et al., 2009; Barchi, 2010). Since late Pliocene these contractional structures have been affected by extensional tectonics (Barchi, 2010; Caricchi et al., 2015). In this sector of the Apennines, crustal extension is accommodated by the Altotiberina low-angle normal fault and its high-angle synthetic and antithetic splays (Barchi et al., 1998a; Barchi et al., 1998b; Boncio et al., 1998).

The Montedoglio dam is located at the north-western edge of the Sansepolcro basin, in the Upper Tiber Valley. The Sansepolcro basin is bounded by NE and SW-dipping normal faults. The main fault is the NE-dipping Anghiari-Città di Castello fault, which bounds the western side of the basin (Fig. 1), and which has controlled the evolution of the Upper Tiber Valley basin since the Early Pleistocene (Brozzetti et al., 2009). The eastern side of the basin is bounded by the SW-dipping Sansepolcro normal fault (Fig. 1). The northern side of the basin has an angular shape, with a relatively linear SW-NE edge controlled by the Montedoglio fault. Deep seismic reflection profiles indicate that the Pliocene-Quaternary continental infill of the Sansepolcro basin is ~1.0–1.2 km-thick (Barchi and Ciaccio, 2009; Mirabella et al., 2011; Pucci et al., 2014). The Tiber River floodplain is characterized by Holocene alluvial sediments, while a Pleistocene fluvio-palustrine sequence and colluvial sediments crop out along the Anghiari ridge, where they are exhumed in the footwall of the main NE-dipping Anghiari fault (Cattuto et al., 1995). From the oldest, the main Lower-Middle Pleistocene stratigraphic units are the Fighille unit, Citerna unit (CTA) and Monterchi unit (MTC). Respectively these units are mostly made of clay and silt, gravel and alternance of sand and fine gravel with a reddish clayey paleosol on top. A series of late Quaternary alluvial fans accumulated along the boundaries of the basin. The bedrock outside the basin is formed by the Jurassic to Lower Eocene ophiolite sequence, to the north, and by the Lower Oligocene to Middle Miocene turbiditic successions of the Tuscan and Umbrian tectonic units, to the west and east (Fig. 1).

The SW-NE-striking Montedoglio fault is reported in the ITHACA database as a capable fault crossing the Montedoglio dam (ITHACA Working Group: ITHACA (ITaly HAzard from CApable Faulting), 2019). The ITHACA fault trace, compiled from Bonini et al. (2016), is reported in Fig. 1. Several authors give different interpretations of its activity status. Cattuto et al. (1995) consider the Montedoglio fault a transfer fault active during the evolution of the basin as well as Delle Donne et al. (2007) and Pucci et al. (2014). Benvenuti et al. (2016) propose that the Montedoglio fault has an important role and facilitates interaction between the main NW-SE-striking normal faults and SW-NE-striking faults. They describe the Montedoglio fault as a continuous 6 km-long SE-dipping normal fault with a dextral component. According to these authors, the Montedoglio fault beheads Middle-Upper Pleistocene alluvial fans and has had an important role in the evolution of the Sansepolcro basin since the Middle Pleistocene.

The Montedoglio dam is located about 1.5 km from the Anghiari normal fault in the hanging wall. According to Testa et al. (2023) the Anghiari fault is an 11 km-long, segmented normal fault displacing Pleistocene to Holocene sediments of the Anghiari ridge. The Anghiari fault is part of the NE-dipping Anghiari-Città di Castello main normal fault. It extends from the Rognosi Mountains to the northern bench of the Sovara River and can be divided into four fault *sections* based on their map pattern and geometric complexities or gaps separating them (Fig. 1). The term "fault section" is used here for purely descriptive

purposes, to avoid using the term "segment" that can be mistaken with "earthquake segment" (i.e., the discrete portion of a fault that ruptures to the surface; see discussion in chapter 9 of McCalpin, 2009). How the sections are interpreted to constitute an earthquake segment will be discussed below (Section 3.5.3 Fault parameters and rupture scenarios). With reference to Fig. 1, the Anghiari – Motina and Fighille sections strike along the base of the eastern side of the Anghiari ridge. The Micciano section is located within the northern Anghiari ridge, at the base of triangular facets. The Valcelle section is in the middle of the southern Anghiari ridge, within a parallel-to-the-ridge valley; its morphologic expression is less prominent among the other fault sections. The Città di Castello fault bounds the western margin of the southern basin, from the southern bank of the Sovara River to the Città di Castello township. The Città di Castello fault does not have a segmented geometry and forms a single fault section (Testa et al., 2023).

The seismogenic behavior of the Anghiari-Città di Castello main fault, considered a synthetic splay of the Altotiberina low-angle normal fault, has been debated for a long time (e.g., Brozzetti et al., 2009 and references therein). Recent paleoseismological investigations (Testa et al., 2023) revealed the Late Pleistocene – historical activity of the Anghiari normal fault and discovered the occurrence of up to seven surface faulting events over the last 25 ka, the recent most of which being consistent with the 1458 Sansepolcro earthquake ($M_w$ 5.8, Mercalli-Cancani-Sieberg epicentral intensity VIII-IX, Rovida et al., 2022). Testa et al. (2023) conclude that the fault can produce moderate to large surface faulting earthquakes (e.g. M > 6). The authors attribute to this fault a slip rate of 0.14–0.35 mm/yr and a maximum magnitude of 6.2, or 6.7 if the whole Anghiari - Città di Castello fault ruptures. These new findings on the activity of the Anghiari fault, and the hanging wall location and proximity to the fault trace, potentially exposes the Montedoglio dam to FDH in case of activation of the Anghiari or Anghiari – Città di Castello faults during a strong earthquake.

## 3. Methods and data

### 3.1. Earthquake geology investigations to constrain fault capability

To constrain the capability of the Montedoglio fault we performed a complete earthquake geology study including field and remote sensing survey, geophysical investigations, core drillings and sample dating. Details on these methods are explained in the Supplementary material (Text S1).

### 3.2. Probabilistic fault displacement hazard analysis

In their pioneering work of PFDHA for assessing the fault displacement hazard of the radioactive waste repository of Yucca Mountains (USA), Youngs et al. (2003) propose two different approaches: the earthquake approach and the displacement approach. While the displacement approach is based on the characteristics of the dislocation observed at the site of interest, the earthquake approach relates the probability of having surface faulting to the probability of having a surface faulting earthquake, in a similar way to the probabilistic method used for assessing the ground shaking seismic hazard (e.g., Cornell, 1968; Cornell, 1971). Instead of ground shaking, the method estimates the likelihood of exceeding a certain value of ground displacement due to principal (on-fault) or distributed (off-fault) faulting. The displacement approach cannot be used because there are no paleoseismic data on the Montedoglio fault. For this reason, we selected the earthquake approach to perform our analysis.

Youngs et al. (2003) remains the only method for normal faulting, although some papers have been published for PFDHA associated with strike-slip and reverse environments (Petersen et al., 2011; Moss and Ross, 2011; Takao et al., 2013; Nurminen et al., 2020). Ferrario and Livio (2021) recently proposed updated regressions for the conditional probability of distributed faulting occurrence as a function of distance from the principal fault for normal faulting environment. For our analyses, we used the earthquake approach by Youngs et al. (2003) integrated with the updated regressions by Ferrario and Livio (2021), computing several hazard curves and their mean to explore the epistemic uncertainties.

#### 3.2.1. Earthquake approach by Youngs et al., 2003

The equation proposed in the earthquake approach by Youngs et al. (2003) to get the exceedance rate of a specific value of displacement in a certain site is the following:

$$V_k(d) = \sum_n \alpha_n(m^0) \int_{m^0}^{m^u} f_n(m) \left[ \int_0^{\infty} f_{kn}(r|m) \bullet P_{kn}{}^{*}(D > d|m,r) \bullet dr \right] \bullet dm$$

Where $V_k(d)$ is the annual rate of exceedance for a given rate of displacement; $\alpha_n(m^0)$ is the occurrence rate of earthquakes with magnitude higher than $m^0$ for a seismogenic source $n$; $f_n(m)$ is the probability density function for earthquakes between $m^0$ and the maximum magnitude $m^u$ associated with the source $n$; $f_{kn}(r|m)$ is the probability density function to have an earthquake of magnitude $m$ at the source $n$ located at a distance $r$ from the site of interest $k$; $P_{kn}{}^{*}(D > d|m,r)$ is the attenuation relation of the displacement and it is made up of two terms:

$$P_{kn}{}^{*}(D > d|m,r) = P_{kn}(Slip|m,r) \bullet P_{kn}(D > d|m,r,Slip) \quad (2)$$

Where $P_{kn}(Slip|m,r)$ is the conditional probability of having displacement occurrence at the site $k$ due to an earthquake of magnitude $m$ on a fault source $n$, the surface trace of which is at a distance $r$ from the site $k$; and $P_{kn}(D > d|m,r,Slip)$ is the conditional distribution of the displacement. Eqs. 1 and 2 can be used for both principal and distributed faulting, considering respectively the position along or the distance from the trace of the principal fault. The probability of occurrence of surface rupturing on the principal fault is a function of magnitude, and it is estimated using a logistic regression for the data provided by Wells and Coppersmith (1993), dePolo (1994) and Pezzopane and Dawson (1996). The probability of exceedance of certain values of displacement along the principal fault rupture is a function of the position along the strike of the fault, and it is estimated using a β function where the displacement is a function of the expected maximum displacement (MD) or the expected average displacement (AD) of the fault under consideration.

The probability of occurrence for distributed faulting has been estimated by Youngs et al. (2003) using the database of surface faulting maps by Pezzopane and Dawson (1996) from the Extensional Cordillera of western USA. Using raster scans of the rupture maps with a pixel size of 0.5 × 0.5 km, the authors computed the rate of occurrence of distributed ruptures for each earthquake by dividing the number of pixels containing distributed ruptures by the total number of pixels within the surface faulting area. Then, the conditional probability was computed using a logistic regression. For estimating the probability of exceedance for a given displacement on distributed ruptures, using the displacement data points collected by dePolo (1994) for five normal faulting earthquakes, Youngs et al. (2003) suggest a distribution of the ratio between the displacement on the distributed rupture and the MD of the principal fault. The distribution is expressed as a function of the distance from the principal fault.

#### 3.2.2. Probability of occurrence of distributed faulting according to Ferrario and Livio (2021)

Ferrario and Livio (2021) updated the database used by Youngs et al. (2003), using data from 21 additional worldwide normal faulting earthquakes, which occurred between 1887 and 2016. They applied the same methodology in Youngs et al. (2003), starting from a raster ruptures map gridded with 0.5 × 0.5 km pixels to obtain the probability of having distributed faulting. This paper used the same logistic distribution used by Youngs et al. (2003):

$$P(x) = \frac{e^{(a+b\bullet(ln(x+c)\ )}}{1+e^{(a+b\bullet(ln\ (x+c)\ )}} \quad (3)$$

Where $x$ is the distance from the principal fault expressed in km and $a$, $b$ and $c$ are coefficients estimated by data (see Table 2 in Ferrario and Livio, 2021): they are a function of the position with respect to the principal fault (footwall or hanging wall) and are independent from earthquake magnitude. These coefficients differ from those proposed by Youngs et al. (2003). Ferrario and Livio (2021) proposed two different regressions (referred to as scenarios) with different $a$, $b$ and $c$ coefficients: i) regular scenario, obtained by fitting both the pixel containing and not containing distributed ruptures; and ii) conservative scenario, obtained by fitting only the pixel containing distributed ruptures. The latter scenario produced a higher probability than the regular one. The authors suggest using both scenarios as two different branches of a logic tree. The curves of conditional probability for distributed faulting obtained by Ferrario and Livio (2021) are higher than the curves proposed by Youngs et al. (2003), especially in the hanging wall of the principal fault, as shown in Fig. 2.

### 3.3. Fault parameters and rupture scenarios

Fault parameters (maximum magnitude, MD, AD) and fault activity rate are crucial input data in the PFDHA. The activity rate, which is the first member of Eq. 1, depends on the fault slip rate. Maximum magnitude, MD and AD depend on the fault geometry and segmentation. As the Anghiari – Città di Castello fault does not have a simple and continuous trace at the surface, its possible segmentation during earthquake faulting is a source of epistemic uncertainty. We took this uncertainty into account by considering different rupture scenarios. Those scenarios involve different combinations of ruptures on different fault sections of the Anghiari fault, also considering the possibility of rupturing the entire Anghiari – Città di Castello main fault. The rupture scenario affects the total length of the rupture, and, therefore, the earthquake magnitude. Moreover, it influences the distance between the dam and the principal fault rupture. We used the MD, AD and slip rates obtained by Testa et al. (2023) and based on field, geophysical and palaeoseismic investigations.

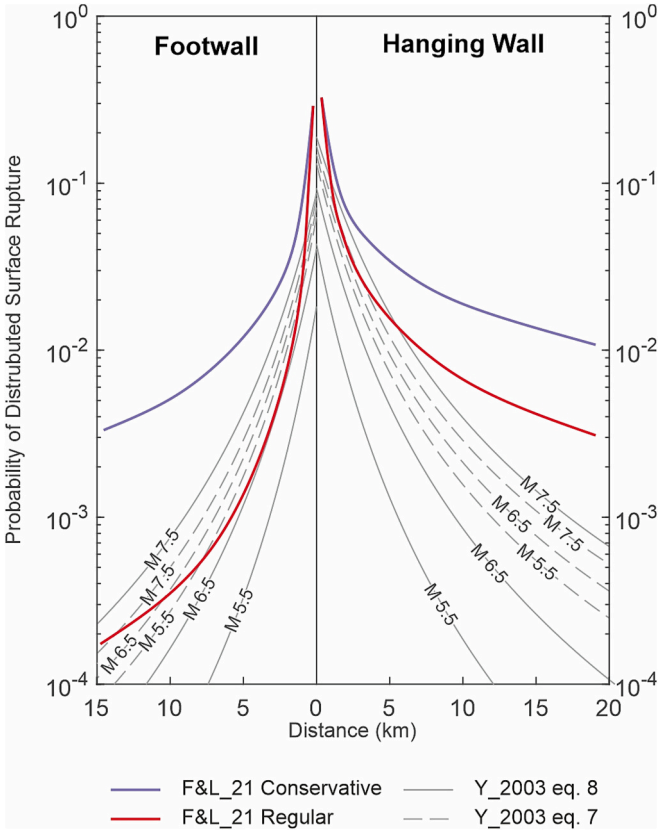


**Fig. 2.** Comparison between the probability of occurrence of distributed faulting, for both footwall and hanging wall, from eqs. 7 and 8 by Youngs et al., 2003 (Y_2003 eq. 7 and Y_2003 eq. 8) for different magnitude (M) classes and Ferrario and Livio, 2021 conservative (F&L_21 Conservative) and regular (F&L_21 Regular) scenarios. Note that the F&L_21's regressions do not depend on earthquake magnitude.

We explore the magnitude uncertainty of each scenario, using the FiSH approach by Pace et al. (2016). The geometry and slip rate data of each rupture scenario have been used to estimate its seismogenic potential. To evaluate the maximum magnitude of each scenario, we first computed and then combined up to four maximum magnitude estimates. Two of these are obtained with the Leonard (2010) empirical relationships for the maximum rupture area (fault dip at depth and seismogenic thickness from Brozzetti et al., 2009) and maximum subsurface rupture length; a third value of maximum magnitude (MAR from aspect ratio) was computed by reducing the fault length for aspect ratio (W/L) smaller than a threshold value derived by Peruzza and Pace (2002); and a fourth value of maximum magnitude (MMo) is based on the calculated scalar seismic moment (M0) and the application of the Hanks and Kanamori (1979) standard formula $Mw = 2/3\ (logM_0 – 9.1)$. It has to be noted that in this case, Pace et al. (2016) assume strain drop equal to $3 \times 10^{-5}$. As each of these four maximum magnitudes is affected by an uncertainty in its estimation, we created a probability curve for each magnitude, assuming that the uncertainty can be described by a normal distribution (Pace et al., 2016). Subsequently, we summed the probability density curves and fitted the summed curve to a normal distribution to obtain a mean of the four magnitudes and a standard deviation. Thus, a unique maximum magnitude with a standard deviation is computed for each scenario, and this value represents the maximum rupture that is allowed by the fault geometry and the seismogenic thickness.

## 4. Results

### 4.1. Principal faulting hazard related to the Montedoglio fault system

Given its status and position in the ITHACA database, the Montedoglio fault constitutes a potential source of fault displacement hazard for the Montedoglio dam. To assess the capability of this fault to nucleate an earthquake and cause surface rupture along its trace, we analyzed this structure by combining the results from geological survey, continuous core drilling, and geophysics.

First order evidence about the activity status of the Montedoglio fault are given by the geological map of the north-western edge of the Sansepolcro basin (Fig. 3), where both the Pleistocene to Holocene continental units and the Jurassic to Eocene marine bedrock crop out. The Montedoglio fault is made of several, nearly parallel, SW-NE to W-E striking high-angle discontinuous faults, distributed over hundreds of meters within ophiolite bedrock (Fig. 3). For this reason, hereinafter, the Montedoglio fault will be referred to as Montedoglio fault system. The trace of the southernmost splay of the Montedoglio fault system crops out along the road to the Montedoglio dam. According to its strike (≈30°N) the projection of this splay intercepts the Montedoglio dam between a half and a third of its length from its right-hand side (NW).

The bedrock of the southern slopes of the Rognosi Mountains is covered by continental deposits such as alluvial terraces of the Tiber River and the older CTA and MTC units. The contact between those latter continental units and the marine bedrock has been interpreted by some authors as a sharp tectonic contact along the Montedoglio fault (Benvenuti et al., 2016; Bonini et al., 2016). Nevertheless, our detailed mapping (Fig. 3) shows that this contact is not as sharp as previously thought, suggesting a stratigraphic unconformity instead of a tectonic contact. At fault outcrops, the prevailing kinematics of the Montedoglio fault system is strike slip, with both normal and reverse components,

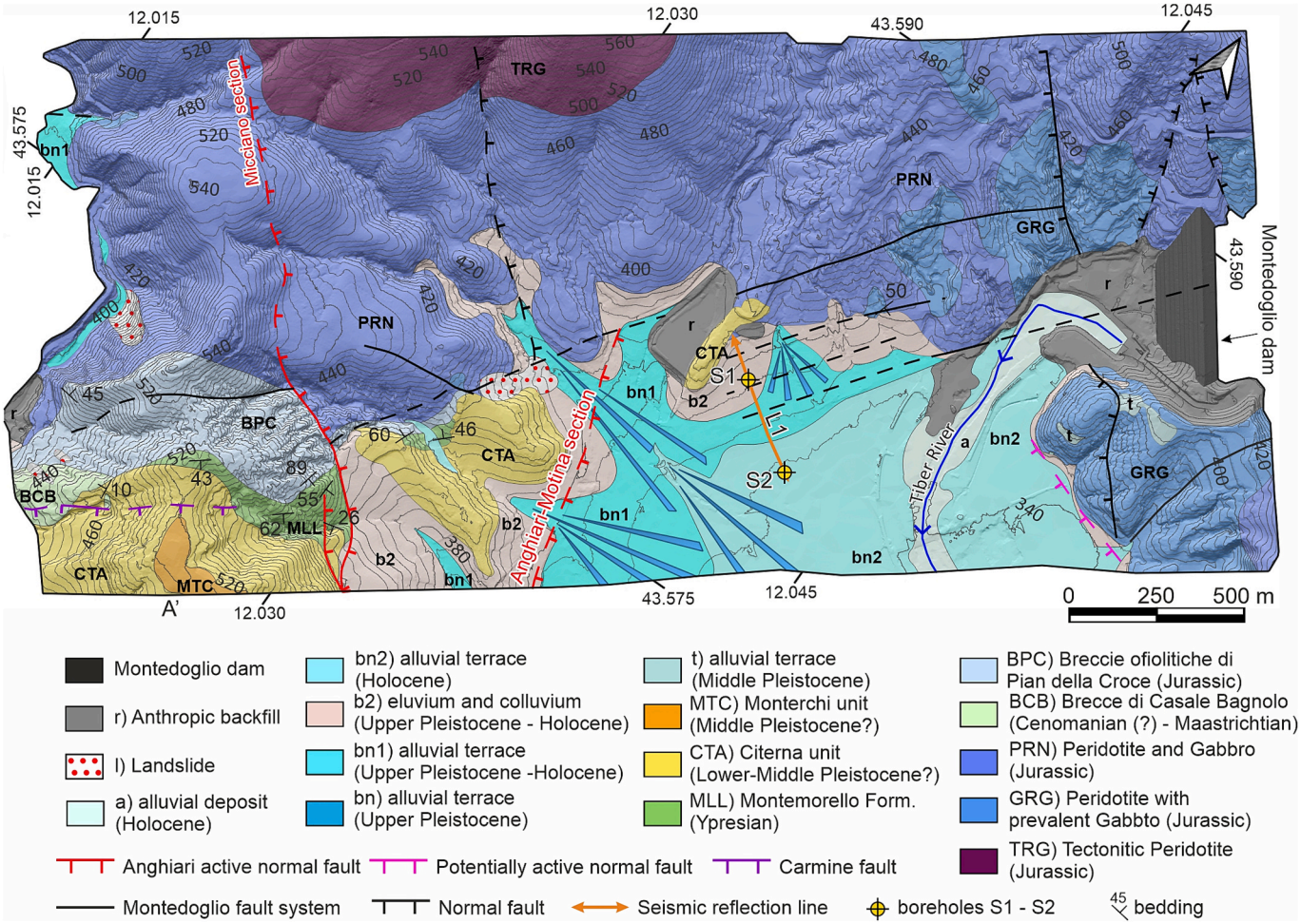


**Fig. 3.** Geological map of the north-western edge of the Sansepolcro basin and location of seismic line L1 and boreholes S1 and S2.

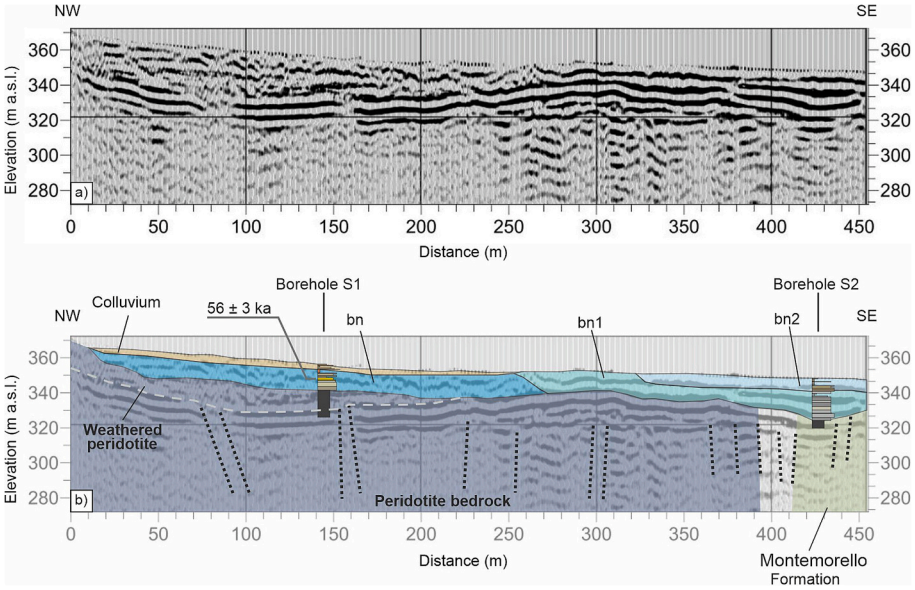


**Fig. 4.** Uninterpreted (a) and interpreted (b) seismic line L1, with the location and stratigraphy of boreholes S1 and S2. bn = Upper Pleistocene alluvial terrace; bn1 = Upper Pleistocene – Holocene alluvial terrace; bn2 = Holocene alluvial deposits. Black dashed lines represent the Montedoglio fault system. Note that the oldest alluvial sediments covering the bedrock are older than 56 ± 3 ka.

with local evidence of reactivations as normal faults.

We acquired a seismic reflection profile extending along a NW-SE direction across the projected trace of the Montedoglio fault system (L1 in Fig. 3 and Fig. 4). The line L1 starts at the junction between the Jurassic bedrock and the alluvial-colluvial cover of the Tiber valley and extends towards the center of the basin. The seismic survey confirms that the Montedoglio fault system is made of several nearly parallel faults.

The seismic line L1 was interpreted thanks to two continuous coring boreholes (S1 and S2 in Fig. 3). Borehole S1 (elevation ~15 m above the Tiber River), located in the northern half of the seismic line L1, drilled about 3 m of ploughed soil, 12 m of alluvial deposits and 15 m of peridotite bedrock. The first upper 3 m of bedrock are deeply weathered, while below 3 m the bedrock is fractured but unweathered. The age of the alluvial deposits was determined by OSL dating of the undisturbed sample C6 to 56 ± 3 ka (Table 1).

Fig. 5a shows a log of borehole S1, the stratigraphy of which is described in detail in Text S2 in the Supplementary material. Borehole S2 (elevation ~6 m above the Tiber River), located close to the southern end of the seismic line L1, drilled about 0.45 m of ploughed soil and two different alluvial units overlying the bedrock. The youngest alluvial unit is 8 m thick and comprises mostly brownish clay and sandy gravel. The oldest alluvial unit has a thickness of 16 m and is made of gravel with gray sandy matrix. The bedrock is characterized by silty and marly layers of the Montemorello Formation (Ypresian). Fig. 5b shows a log of the borehole S2, the stratigraphy of which is described in detail in Text S2 in the Supplementary material.

Our interpretation of the seismic line L1 (Fig. 4b) depicts a Montedoglio fault system that does not displace the Upper Pleistocene to Holocene alluvial deposits (bn and bn1 in Fig. 3). In this interpretation, those deposits seal the fault zone. Actually, the contact between the bedrock and the overlaying continental units is almost flat, without steps, steep slopes, or abrupt thickening of the above continental succession.

This data set leads us to conclude that the Montedoglio fault system does not affect the continental deposits, the oldest part of which is older than 56 ± 3 ka.

The geological survey also highlighted the presence of a SSE-dipping fault, known as Carmine fault (Benvenuti et al., 2016). This latter fault displaces the unconformity between the Citerna continental sediments and the underlying ophiolite bedrock for a few decimeters (Fig. S1 in the Supplementaty material). The fault zone has both right-lateral and normal slip indicators. The fault has a limited length and there is no evidence of continuation towards the NE. Therefore, the Carmine fault seems to be a secondary structure that is less important than previously thought.

### 4.2. Distributed faulting hazard related to the Anghiari - Città di Castello main fault

The hazard related to secondary (distributed) ruptures linked to nearby primary faults cannot be excluded. In fact, the dam is close (~1.5 km) to the active and capable Anghiari - Città di Castello main normal fault (Testa et al., 2023). Moreover, the Montedoglio dam is located within the hanging wall of this fault. It is known that the hanging wall has higher probability of distributed ruptures than the footwall, even at large distances from the principal fault (Youngs et al., 2003; Boncio et al., 2012; Ferrario and Livio, 2021). It is also possible that the pre-existing discontinuities within the ophiolitic bedrock of the Montedoglio fault system could be partially reactivated in the form of secondary faulting, even though their orientation is not optimal compared to the general trend of the active strain (NE-directed extension). Moreover, brittle cataclastic reactivation as dip-slip normal faults was discontinuously observed in the Montedoglio fault system, leading us to estimate the probability of having distributed faulting following a probabilistic approach.

#### 4.2.1. Rupture scenarios

A map of the fault traces forming the Anghiari - Città di Castello main fault, and four possible rupture scenarios considered in this work for the probabilistic analysis of fault displacement hazard are imaged in Fig. 6. In the same figure, we show the total length of the principal rupture, the minimum distance from the dam, the maximum magnitude (discussed in the next paragraph) and the sites where the slip rates have been measured by Testa et al. (2023). The fault parameters for each scenario and the minimum distance from the dam are listed in Table 2.

The seismogenic depth and the average dip of the fault have been inferred considering the interpretation of seismic reflection data (Brozzetti et al., 2009) and the dip of the fault at the surface.

#### 4.2.2. Maximum magnitude and activity rates

The output of the MB Tool of the software FiSH (Pace et al., 2016), with the maximum magnitude computed for each scenario are shown in Fig. S2 of the Supplementary material. The computed maximum magnitude for the four scenarios from 1 to 4 are respectively 6.3 (+ − 0.3), 6.6 (+ − 0.3), 6.2 (+ − 0.3), and 6.6 (+ − 0.3).

The expected activity rates (Fig. S3 in the Supplementary material) have been computed for each scenario using a Characteristic Gaussian Magnitude-Frequency distribution (MFD) model that considers a symmetric Gaussian curve (applied to the incremental MFD values) centered on the maximum expected magnitude value of each scenario with a range of magnitudes equal to 1-sigma. These rates have been used to solve the first term of eq. (1) by Youngs et al. (2003).

#### 4.2.3. Probabilistic Fault Displacement Hazard Analysis (PFDHA)

The results of the PFDHA are expressed in terms of hazard curves (Fig. 7a) of annual frequency of exceedance (AFOE, vertical axis) of the vertical component of dip-slip normal displacement values (horizontal axis) at the site of the dam. For each scenario (colored curves in Fig. 7a) three curves have been computed using the equations of Youngs et al. (2003) (dotted curves in Fig. 7a), the equation by Youngs et al. (2003) integrated with the equation of the regular scenario by Ferrario and Livio (2021) (dashed curves in Fig. 7a) and the equation by Youngs et al. (2003) integrated with the equation of the conservative scenario by Ferrario and Livio (2021) (continuous curves in Fig. 7a). In order to account for the epistemic uncertainty related to the selection of rupture scenarios and selection of equations, the average curve, with equal weights for each scenario, and the percentiles 2.5 and 97.5 have been computed (Fig. 7b).

The mean hazard curve is always below an AFOE of $1 \times 10^{-5}$. The return period (1/AFOE) of a rupture with a displacement <1 cm at the dam's site is >100,000 years. The percentile 97.5 intercepts the value of AFOE of $1 \times 10^{-5}$ corresponding to a displacement of 6 cm. This means that the return period of a rupture with a displacement of 6 cm at the site is in the order of 100,000 years.

Setting a hypothetical critical value of 10 cm of displacement, the corresponding AFOE ranges from $1 \times 10^{-6}$ to $6 \times 10^{-6}$, with a mean value of $3 \times 10^{-6}$, which corresponds to a return period of about 150,000–760,000 years with a mean value of about 320,000 years. Given that the probability of exceedance corresponds to the ratio

**Table 1**
Results of the OSL dating of sample C6. $ED_{CAM}$ (Gy) = equivalent dose, central age model; DR (Gy/ka) = dose rate.

| Sample name | Long. | Lat. | Depth (m) | Dated material | Method - Lab. | Date of sampling (d/m/y) | $ED_{CAM}$ (Gy) | DR (Gy/ka) | $Age_{CAM}$ (ka) |
|---|---|---|---|---|---|---|---|---|---|
| C6 | 12.0395 E | 43.5804 N | 8 | Fluvial sand | PH3DRA Catania, Italy | 24/05/2021 | 108 ± 6 | 1.9 ± 0 0.1 | 56 ± 3 |

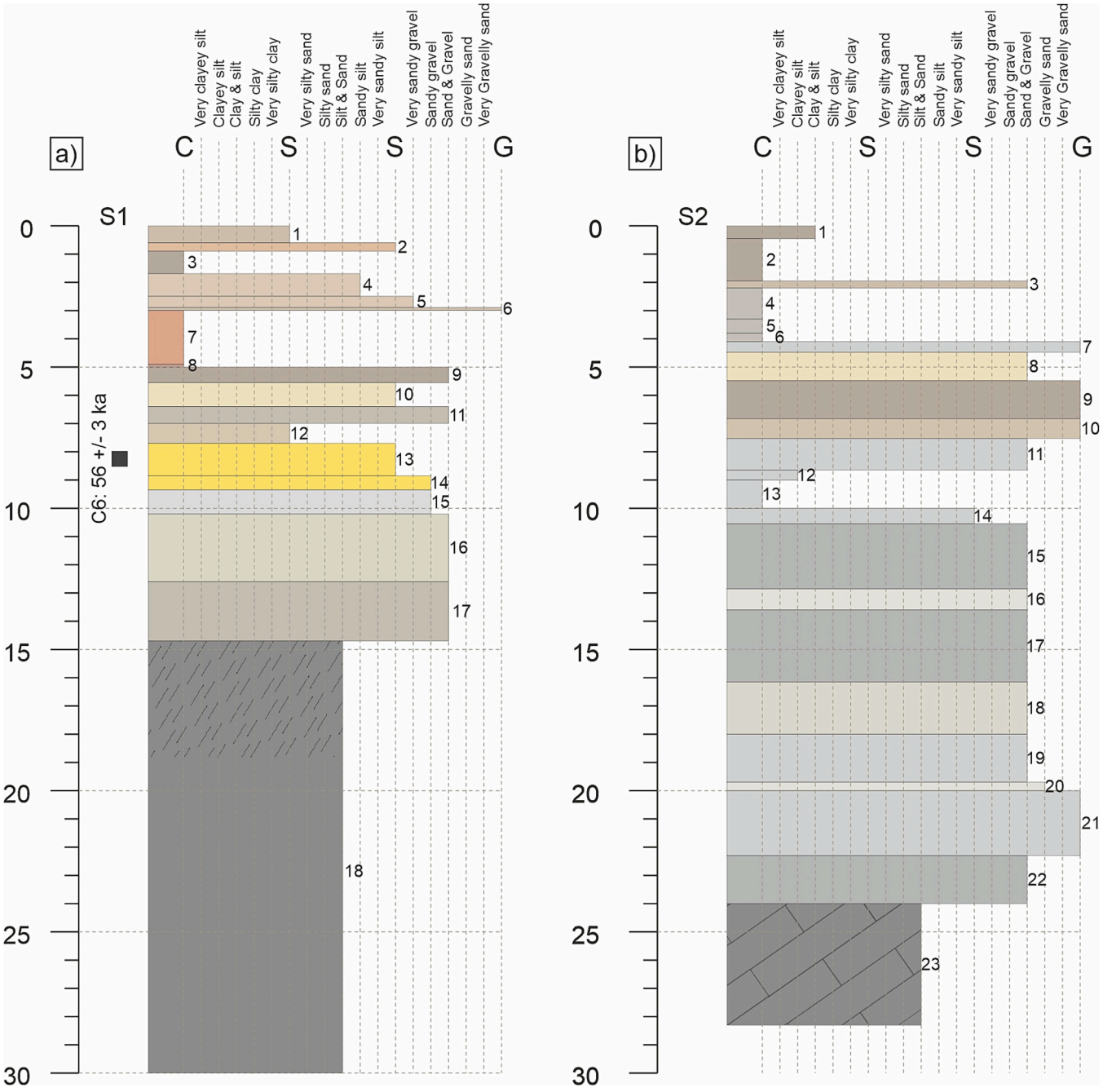


**Fig. 5.** Stratigraphy of the boreholes S1 (a) and S2 (b). Progressive numbering of the sedimentary layers refers to the detailed stratigraphic description in Text S1 of the Supplementary material.

between the expected life of an infrastructure (200 years for a strategic dam according to DMIT, 2014) and the return period, the probability of exceedance of 10 cm of displacement in 200 years ranges from 0.13 % to 0.03 % with an average value of 0.06 %.

## 5. Discussion

### 5.1. Montedoglio fault system

The geological and geophysical investigation results indicate that the Montedoglio fault is not a single and continuous 6 km-long fault as compiled in the ITHACA database from Benvenuti et al. (2016) and Bonini et al. (2016). We found several discontinuous and nearly parallel SW-NE striking faults within ophiolite bedrock, forming a system of parallel faults (Montedoglio fault system). The geological survey highlights also that the faults belonging to the Montedoglio system have experienced different kinematic phases.

We did not find convincing evidence of tectonic subsidence at the hanging wall of the Montedoglio fault system during the deposition of continental units, suggesting that the control of this fault system on the evolution of the basin is not as important as previously thought. The relatively sharp termination of the basin along the SW-NE lineation, obvious when observing the basin at a small scale (e.g., Fig. 1), can derive from the convergence of structural and morphological factors, such as the presence of a wide, ancient, exhumed fault zone, high erodibility of the bedrock along the fault zone and partial reactivations during the early stages of the basin formation.

The seismic reflection survey combined with the boreholes and the

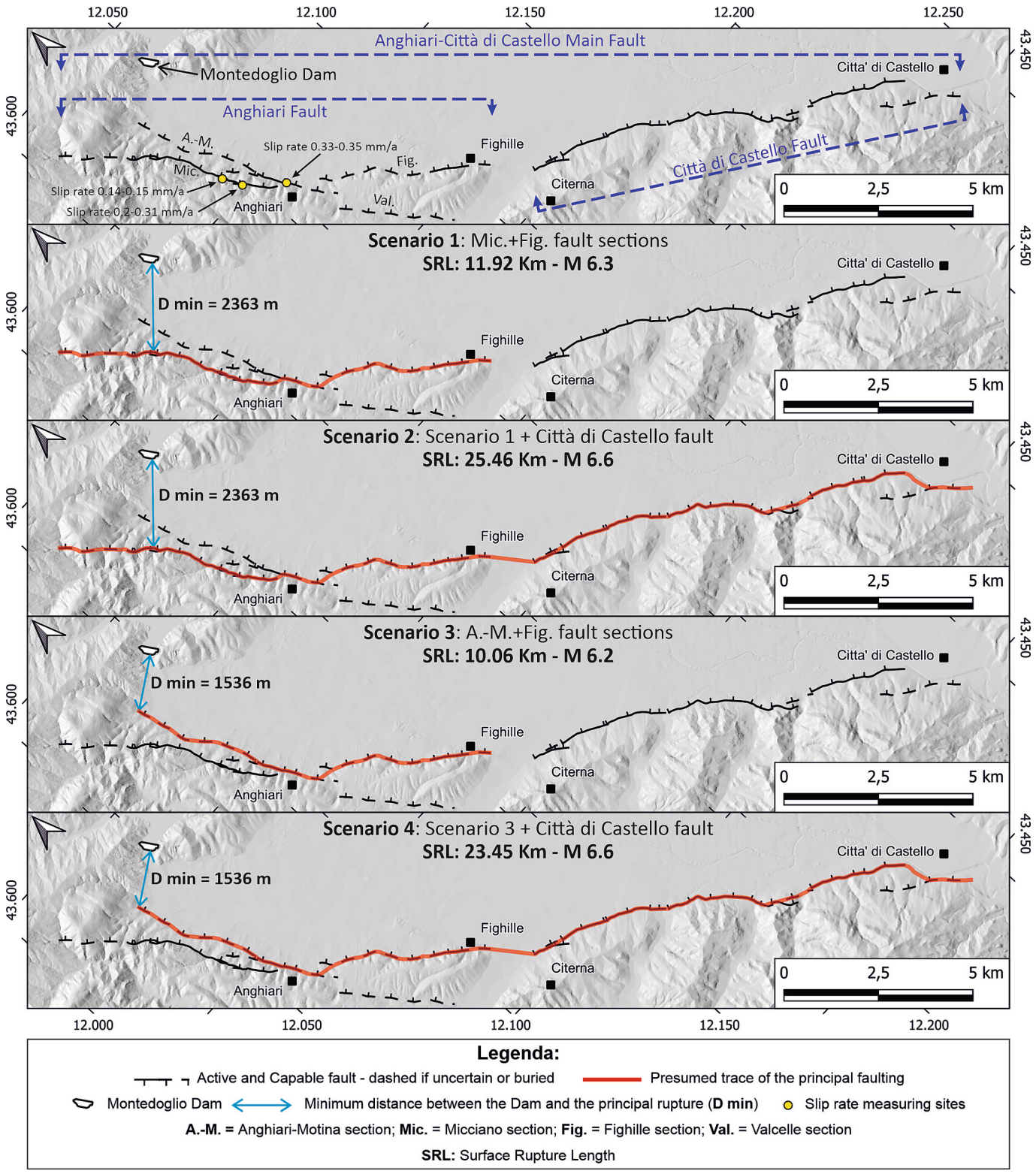


**Fig. 6.** Detailed segmentation map of the Anghiari-Città di Castello main fault and the four rupture scenarios used for the PFDHA analysis.

OSL dating confirm that the Montedoglio fault system is sealed by undisturbed alluvial deposits ≥56 ± 3 ka old.

The only evidence of displacement of continental deposits along the Montedoglio system is the Carmine fault cited in Benvenuti et al. (2016) (Fig. S1 in the Supplementary material). The Carmine fault accommodates small displacement (a few decimeters) of the Citerna unit, of uncertain age but probably of Early or Middle Pleistocene age (Pialli et al., 2009; Pucci et al., 2014).

All these lines of evidence suggest that the Montedoglio fault system has an ancient displacement history with partial reactivation as secondary faults during the early stage of basin formation, and it has been inactive since more than 50 ka. Considering the 40 ka thresholds from the Italian guidelines for seismic microzonation (SM Working Group, 2015), the Montedoglio fault system cannot be classified as capable.

**Table 2**
Summary of the fault parameters for each rupture scenario. MD and AD came from the empirical regressions by Wells and Coppersmith (1994) taking the average among the expected values for both normal faulting environment and all the kinematics.

| Scenario | Length (Km) | Average Dip (°) | Seismogenic depth (Km) | Slip rate min / max (mm/anno) | Mmax | MD (m) | AD (m) | Minimum distance from the Dam (m) |
|---|---|---|---|---|---|---|---|---|
| 1 | 11,92 | 40 | 7 | 0.14/0.35 | 6.3 ± 0.3 | 0.5 | 0.3 | 2363 |
| 2 | 25,46 | 40 | 7 | 0.14/0.35 | 6.6 ± 0.3 | 0.9 | 0.5 | 2363 |
| 3 | 10,6 | 40 | 7 | 0.14/0.35 | 6.2 ± 0.3 | 0.4 | 0.3 | 1536 |
| 4 | 23,45 | 40 | 7 | 0.14/0.35 | 6.6 ± 0.3 | 0.9 | 0.5 | 1536 |

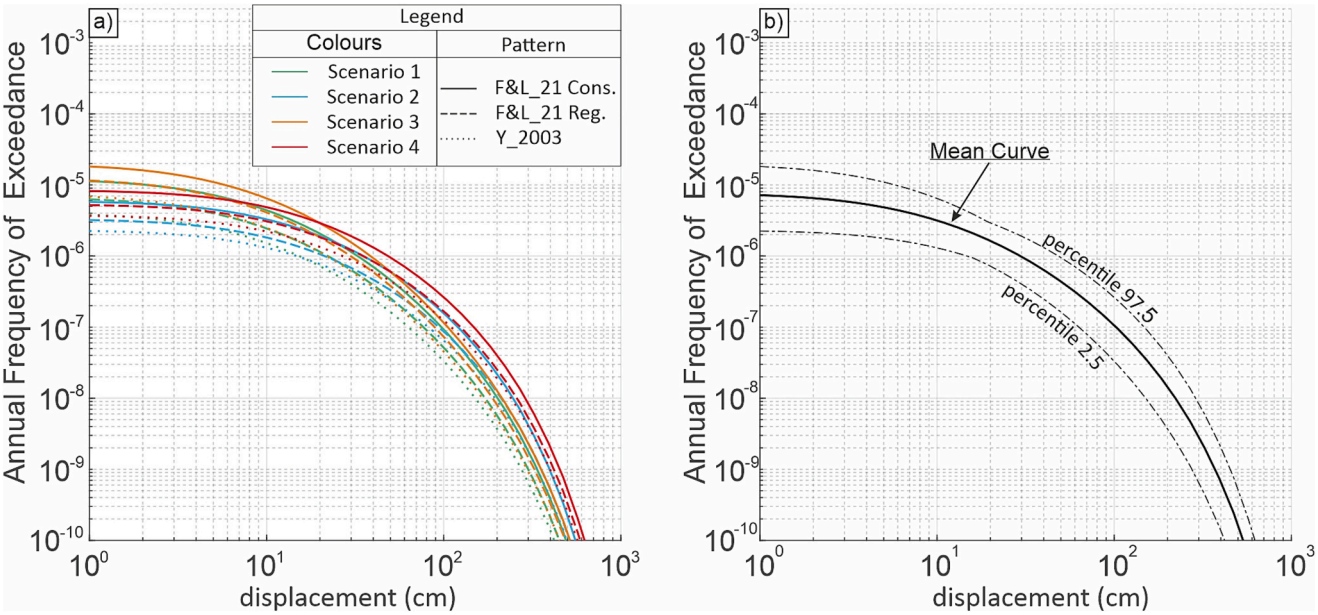


**Fig. 7.** a) Curves of distributed displacement hazard at the site of the Montedoglio dam, computed for each scenario (colors) and for each function; continuous curves (F&L_21 Cons.) = Ferrario and Livio, 2021 - Conservative; dashed curves (F&L_21 Reg.) = Ferrario and Livio, 2021 - Regular; dotted curves (Y_2003) = Youngs et al., 2003; b) average curve of distributed displacement hazard at the site of the dam, obtained by averaging all the scenarios and functions, and the 2.5 and 97.5 percentiles, corresponding to the lower and upper boundary of all the curves plotted together.

According to International Atomic Energy Agency (IAEA) (2022), in highly active areas, with short earthquake recurrence intervals, a fault should be considered capable if there is evidence of past movements in the Late Pleistocene to the Holocene. Even though the unfaulted stratigraphic succession is not as old as the entire Late Pleistocene, this evidence is not sufficient to consider the fault as potentially capable. In fact, in the Italian Apennines, paleoseismologic studies suggest that the maximum recurrence intervals of active normal faults are much shorter than 50 ka (2000 ± 1000 years; Galli et al., 2008; Testa et al., 2023). Moreover, 50 ka is also longer than the longest period of quiescence (anticluster) documented for active normal faults with uneven slip behavior in central Italy (≈10 ka; Mildon et al., 2022).

The previous considerations suggest that the occurrence of a strong earthquake capable of producing principal faulting along the Montedoglio fault system is unlikely.

### *5.2. Fault displacement hazard at the Montedoglio dam site and implications for PFDHA methodology*

Even if the Montedoglio fault system cannot be considered a source of principal surface faulting hazard, the proximity (about 1.5 km, in the hanging wall) of the capable Anghiari fault suggests that distributed faulting at the dam site cannot be excluded. In addition, the pre-existing discontinuities of the Montedoglio fault system could be reactivated as secondary hanging wall ruptures upon nucleation of a strong earthquake on the principal fault (Anghiari fault). In the literature, there are several examples of the occurrence of distributed faulting up to tens of kilometers from the principal rupture (Nurminen et al., 2022), the most recent one in an extensional setting being the 2016 Mw 6.5 normal faulting earthquake in Central Italy (Civico et al., 2018).

The occurrence of distributed faulting along pre-existing discontinuities is not directly addressed by Youngs et al. (2003). In fact, Youngs et al. (2003) deal with the probability of having distributed faulting with an independent function, discarding the nature of the ruptures, and considering all the secondary ruptures without any distinction. The authors investigate the influence of the angle θ between the strike of the principal rupture and the strike of the secondary discontinuities on the probability of distributed faulting. They suggest that the probability of occurrence of distributed ruptures decreases with increasing θ from 0 to 90°. Being almost orthogonal to the Anghiari fault, the Montedoglio fault system has the most unfavorable orientation for the occurrence of distributed faulting. However, this is an independent relation, and it is not involved in the general equation (Eq. 1). We decided not to consider the dependence on θ in favor of safety.

The near surface geology is another factor that can affect the probability of occurrence of distributed faulting, which is not considered in the current PFDHA methods. For this reason, new empirical models providing different probabilities of occurrence of distributed faulting as a function of the fault ranking (i.e., randomly distributed unexpected ruptures vs reactivation of known pre-existing discontinuities; Nurminen et al., 2022) and different near surface geological conditions should be explored in the future.

To improve the poorly constrained prediction equations (based on the very old database of few cases proposed by Pezzopane and Dawson,

1996) for the probability of having distributed faulting, we integrate the method by Youngs et al. (2003) with the newly released relationships proposed by Ferrario and Livio (2021). However, this choice only addresses the computation of the probability of occurrence of secondary faulting, regardless of the distributed displacement attenuation with distance. Further implementation of this method should address this issue, using databases of coseismic ruptures populated with a robust number of displacement data points (e.g., Sarmiento et al., 2021, 2024a, 2024b; Nurminen et al., 2022).

The probability of exceeding a certain value of displacement for distributed rupture, in Youngs et al. (2003) is expressed as the distribution of the ratio between the distributed displacement and the maximum displacement on the principal fault. However, this approach may not be appropriate when the infrastructure is located close to the tip of the fault (such as for the Montedoglio dam) or, in any case, far from the maximum displacement point. For this reason, new and updated regressions considering along-strike variations of the principal fault displacement are needed.

Being a function of the maximum displacement on the principal fault, the distributed displacement depends on the earthquake magnitude, which in turn depends on the length of the rupture. Considering also that the distance between the infrastructure and the main fault strongly affects the results of PFDHA, detailed fault mapping is a fundamental requisite for this kind of study. For segmented structures (such as the Anghiari fault), the minimum distance from the principal fault depends on which fault sections are involved in the rupture. For this reason, we considered these epistemic uncertainties using different rupture scenarios for the principal rupture, and we suggest this approach is appropriate for similar studies.

Fig. 7a shows twelve hazard curves obtained by computing three curves for each scenario. The three curves relate to the probability of occurrence of distributed surface rupturing obtained with: i) the equation by Youngs et al. (2003) and, ii) the two equations by Ferrario and Livio (2021). Instead of selecting one of those, we suggest estimating the hazard using the mean curve and its uncertainty (2.5 and 97.5 percentiles).

Lastly, we highlight some challenges in communicating the results to decision-makers, and issues with understanding what thresholds are required to inform precautionary decision making. In the literature, and even in local regulations or guidelines, it is difficult to find clear thresholds related to the admissible fault displacement hazard level for a critical infrastructure, such as a dam. A partial exception is given by the Federal Guidelines for Dam Safety – Earthquake Analyses and Design of Dams in force in the USA (Federal Emergency Management Association (FEMA), 2015). Here, there is a reference to a time range of 100,000–35,000 years for classifying a fault as active when determining the maximum credible earthquake for high-hazard dams. In particular, fault movement within the range of 100,000–35,000 years before present is considered recent enough to warrant an active or capable fault classification. Following this indication, one could consider that time range of $10^5$ years would be a reasonably long interval for defining the largest reference return period for admissible fault displacement hazard. The return periods obtained in the present study are longer than the threshold of 100,000–35,000 years (only the percentile 97.5 intercepts the 100,000 years of return period for displacement value = 6 cm). Therefore, the results suggest reasonably acceptable hazard values for the infrastructure under consideration. Apart from the numerical results, the experience from this study indicates that local national authorities, in Italy or elsewhere, should provide indications for AFOE thresholds of fault displacement. Currently, only AFOE thresholds for ground shaking are provided. This will facilitate the usage of PFDHA in earthquake engineering geology practice and will help infrastructure operators and risk managers in their actions.

## 6. Conclusions

We completed a multidisciplinary fault displacement hazard analysis of the Montedoglio fault (sensu ITHACA database), hypothesized to cross the Montedoglio strategic dam. Fault displacement hazard due to principal faulting at the dam's site is unlikely, since the Montedoglio fault is a system of short and discontinuous, old bedrock faults cropping out only within the Jurassic ophiolites and not displacing sediments older than 56 ka. Therefore, the Montedoglio fault system cannot be considered a principal capable fault, able to generate large surface faulting earthquakes. However, secondary (distributed) faulting related to the Anghiari fault, including the possibility of reactivation of pre-existing discontinuities (Montedoglio fault system), cannot be excluded.

The fault displacement hazard at the site of the Montedoglio dam due to secondary faulting has been estimated with a PFDHA approach enhanced with the most updated regressions for extensional settings. The results show that the hazard at the dam's site is low. In fact, the mean hazard curve is always below AFOE $1 \times 10^{-5}$, corresponding to return periods of >100,000 years for displacement values <1 cm. This is the first application of a PFDHA study to an existing dam in Italy, and the results might be of practical interest for future studies, in Italy and elsewhere. Some improvements in the development of the PFDHA method are needed to account for weaknesses of the method and reduce epistemic uncertainties. Particularly, it would be ideal to have different regressions, which distinguish between randomly distributed faulting and reactivation of pre-existing secondary structure which can be mapped before the earthquake. Nurminen et al. (2020), using a ranking of the distributed ruptures into different categories (e.g., 'primary distributed ruptures', referring to reactivation of pre-existing faults that can be mapped before the earthquake, and 'simple distributed ruptures', referring to unpredictable surface ruptures), proposed regressions only for the simple distributed ruptures. Moreover, to improve the evaluation of the expected displacement we would need more sophisticated approaches to model the variability of displacement along the principal fault instead of solely focusing on the maximum or average displacement. The regressions for the distributed displacement attenuation are still poorly constrained by empirical data and new updated models based on numerous observational data are needed. These improvements will facilitate the usage of PFDHA in earthquake engineering geology practice.

Only an integrated approach involving geology-based quantification of the hazard and engineering-based quantification of risk thresholds will lead to a risk-based decision for the safety of infrastructure located near capable faults. Future research developments in this field, together with the synergy of engineering and geology, are needed to achieve advances in the safety of strategic infrastructure systems which are particularly sensitive to FDH.

## Financial support

This work was funded by "Ente Acque Umbre Toscane (EAUT), Arezzo, Italy", which is warmly acknowledged (Conventions 2019 and 2020 between EAUT and Universities of Chieti - Pescara - Resp.: P. Boncio, code CT-EAUT-MONTEDOGLIO - and Perugia - Resp.: F. Mirabella, codes MIRF2019EAUT and MIRFEAUT2021).

## CRediT authorship contribution statement

**Alessio Testa:** Writing – review & editing, Writing – original draft, Visualization, Validation, Methodology, Investigation, Formal analysis, Conceptualization. **Paolo Boncio:** Writing – review & editing, Writing – original draft, Validation, Investigation, Conceptualization. **Bruno Pace:** Writing – review & editing, Writing – original draft, Validation, Methodology, Investigation, Formal analysis, Conceptualization. **Cristina Pauselli:** Writing – review & editing, Writing – original draft, Validation, Investigation. **Maurizio Ercoli:** Writing – review & editing,

Writing – original draft, Visualization, Validation, Investigation. **Eugenio Auciello:** Validation, Investigation. **Francesco Visini:** Methodology, Formal analysis. **Stéphane Baize:** Writing – review & editing, Writing – original draft, Validation, Investigation.

## Declaration of competing interest

The authors declare that they have no known competing financial interests or personal relationships that could have appeared to influence the work reported in this paper.

## Data availability

The Anghiari fault parameters used in the probabilistic fault displacement hazard analysis are from Testa et al., 2023. All the other datasets presented in this study are included in the article and in the Supplementary material.

## Acknowledgements

We are grateful to the Editor Wenping Gong, and the three anonymous reviewer who have significantly improved the quality and readability of our manuscript with their suggestions and comments.

We acknowledge Stefano Pucci, Lucilla Benedetti and Magali Reisner for the fruitful discussion on the active tectonic settings of the area, and Alessandro Valentini for the discussion on probabilistic fault displacement hazard methodology. We also thank the "Ente Acque Umbre Toscane (EAUT), Arezzo, Italy" for the logistic support during geological and geophysical investigations.

## Appendix A. Supplementary data

Supplementary data to this article can be found online at https://doi.org/10.1016/j.enggeo.2024.107817.

## References

Baize, S., Nurminen, F., Sarmiento, A., et al., 2019. A worldwide and unified database of surface ruptures (SURE) for fault displacement hazard analyses. Seismol. Res. Lett. 91 (499–520), 2019. https://doi.org/10.1785/0220190144.

Barchi, M.R., 2010. The Neogene-Quaternary evolution of the Northern Apennines: crustal structure, style of deformation and seismicity. J. Virtual Explor. https://doi.org/10.3809/jvirtex.2009.00220.

Barchi, M.R., Ciaccio, M.G., 2009. Seismic images of an extensional basin, generated at the hanging wall of a low-angle normal fault: the case of the Sansepolcro basin (Central Italy). Tectonophysics 479 (3–4), 285–293. https://doi.org/10.1016/j.tecto.2009.08.024.

Barchi, M.R., De Feyter, A., Magnani, M.B., Minellig Pialli, G., Sotera, B.M., 1998b. Extensional tectonics in the Northern Apennines (Italy): evidence from the CROP03 deep seismic reflection line. Mem. Soc. Geol. It. 52, 527–538.

Barchi, M., Minelli, G., Pialli, G., 1998a. The CROP 03 Profile: a synthesis of results on deep structures of the Northern Apennines. Mem. Soc. Geol. It. 52, 383–400. https://doi.org/10.4236/ijg.2017.811075.

Basili, R., D'Amico, V., Meletti, C., Valensise, G., 2017. Linee-guida per la redazione e le istruttorie degli studi sismotettonici relativi alle grandi dighe. In: INGV, Relazione per ENEL. Accordo ai sensi dell'art. 15 della l. 241/90 e succ. modd. tra la Direzione Generale per le Dighe e le Infrastrutture Idriche ed Elettriche del Ministero delle Infrastrutture e dei Trasporti e l'Istituto Nazionale di Geofisica e Vulcanologia per la redazione di linee-guida per gli studi sismotettonici finalizzati alla rivalutazione della pericolosità sismica dei siti delle grandi dighe. Roma.

Benvenuti, M., Bonini, M., Moroni, A., 2016. Tectonic control on the late Quaternary hydrography of the Upper Tiber Basin (Northern Apennines, Italy). Geomorphology 269, 85–103. https://doi.org/10.1016/j.geomorph.2016.06.017.

Boncio, P., Brozzetti, F., Ponziani, F., Barchi, M., Lavecchia, G., Pialli, G., 1998. Seismicity and extensional tectonics in the northern Umbria–Marche Apennines. Mem. Soc. Geol. Ital. 52, 539–555.

Boncio, P., Galli, P., Naso, G., Pizzi, A., 2012. Zoning surface rupture hazard along normal faults: insight from the 2009 Mw 6.3 L'Aquila, Central Italy, earthquake and other global earthquakes. B. Seismol. Soc. Am. 102, 918–935. https://doi.org/10.1785/0120100301.

Bonini, M., Corti, G., Delle, Donne D., Sani, F., Piccardi, L., Vannucci, G., Genco, R., Martelli, L., Ripepe, M., 2016. Seismic sources and stress transfer interaction among axial normal faults and external thrust fronts in the Northern Apennines (Italy): a working hypothesis based on the 1916–1920 time–space cluster of earthquakes. Tectonophysics 680, 67–89. https://doi.org/10.1016/j.tecto.2016.04.045.

Brozzetti, F., Boncio, P., Lavecchia, G., Pace, B., 2009. Present activity and seismogenic potential of a low-angle normal fault system (Cittá di Castello, Italy): Constraints from surface geology, seismic reflection data and seismicity. Tectonophysics 463, 31–46. https://doi.org/10.1016/j.tecto.2008.09.023.

Bryant, W.A., Hart, E.W., 2007. Fault-rupture hazard zones in California: Alquist–Priolo earthquake fault zoning act with index to earthquake fault zones maps. Calif. Geol. Surv., Spec. Pub. 42, 41.

Caricchi, C., Aldega, L., Barchi, M.R., Corrado, S., Grigo, D., Mirabella, F., Zattin, M., 2015. Exhumation patterns along shallow low-angle normal faults: an example from the Altotiberina active fault system (Northern Apennines, Italy). Terra Nova 27, 312–321. https://doi.org/10.1111/ter.12163.

Cattuto, C., Cencetti, C., Fisauli, M., Gregori, L., 1995. I bacini Pleistocenici di Anghiari e Sansepolcro nell'alta valle del Tevere. Il Quaternario 8, 119–128.

Cheng, Y., Akkar, S., 2017. Probabilistic permanent fault displacement hazard via Monte Carlo simulation and its consideration for the probabilistic risk assessment of buried continuous steel pipelines. Earthq. Eng. Struct. Dyn. 46, 605–620. https://doi.org/10.1002/eqe.2805.

Civico, R., Pucci, S., Villani, F., Pizzimenti, L., De Martini, P.M., Nappi, R., Open Open EMERGEO Working Group, 2018. Surface ruptures following the 30 October 2016 Mw 6.5 Norcia earthquake, Central Italy. J. Maps 14 (2), 151–160. https://doi.org/10.1080/17445647.2018.1441756.

Cornell, A., 1968. Engineering seismic risk analysis. Bull. Seismol. Soc. Am. 58, 1583–1606. https://doi.org/10.1785/BSSA0580051583.

Cornell, A., 1971. Probabilistic analysis of damage to structures under seismic loads. In: Dynamic Waves in Civil Engineering: Proceedings of a Conference Organized by the Society for Earthquake and Civil Engineering Dynamics. John Wiley, New York, pp. 473–493.

Delle Donne, D., Piccardi, L., Odum, J.K., Stephenson, W.J., Williams, R.A., 2007. High-resolution shallow reflection seismic image and surface evidence of the Upper Tiber Basin active faults (Northern Apennines, Italy). Boll. Soc. Geol. Ital. 126 (2), 323–331.

dePolo, C.M., 1994. - The maximum background earthquake in the basin and range. Bulletin of the Seismological Society of America 84, 466–472.

Di Naccio, D., Famiani, D., Liberi, F., Boncio, P., Cara, F., De Santis, A., Di Giulio, G., Galadini, F., Milana, G., Rosatelli, G., Vassallo, M., 2020. Site effects and widespread susceptibility to permanent coseismic deformation in the Avezzano town (Fucino basin, Central Italy): constraints from detailed geological study. Eng. Geol. 270, 105583. https://doi.org/10.1016/j.enggeo.2020.105583.

DMIT, 2014. Norme tecniche per la progettazione e la costruzione degli sbarramenti di ritenuta (dighe e traverse). In: Ministero delle Infrastrutture e dei Trasporti, Decreto 26 giugno 2014, Gazzetta Ufficiale della Repubblica Italiana N. 156 8-7-2014. www.gazzettaufficiale.it.

Federal Emergency Management Association (FEMA), 2015. Federal Guidelines for Dam Safety – Earthquake Analyses and Design of Dams, p. 75.

Ferrario, M.F., Livio, F., 2021. Conditional probability of distributed surface rupturing during normal-faulting earthquakes. Solid Earth 12, 1197–1209. https://doi.org/10.5194/se-12-1197-2021.

Galli, P., Galadini, F., Pantosti, D., 2008. Twenty years of paleoseismology in Italy. Earth Sci. Rev. 88 (1–2), 89–117. https://doi.org/10.1016/j.earscirev.2008.01.001.

Görüm, T., Tanyas, H., Karabacak, F., Yılmaz, A., Girgin, S., Allstadt, K.E., Süzen, M.L., Burgi, P., 2023. Preliminary documentation of coseismic ground failure triggered by the February 6, 2023 Türkiye earthquake sequence. Eng. Geol. 327 (2023), 107315. https://doi.org/10.1016/j.enggeo.2023.107315.

Hanks, T.C., Kanamori, H., 1979. A moment-magnitude scale. J. Geophys. Res. 84, 2348–2350. https://doi.org/10.1029/JB084iB05p02348.

Hosseini, M., Rahimi, H., 2022. Probabilistic fault displacement hazard analysis for the North Tabriz fault. Nat. Hazards Earth Syst. Sci. 22 (11), 3571–3583. https://doi.org/10.5194/nhess-22-3571-2022.

Iezzi, F., Boncio, P., Testa, A., Di Giulio, G., Vassallo, M., Cara, F., Milana, G., Galadini, F., Giaccio, B., De Luca, M., 2023. A case study of multidisciplinary surface faulting assessment in the Urbanized Fucino Basin, Italy. Ital. J. Geosci. 142 (1), 104–121. https://doi.org/10.3301/IJG.2023.03.

International Atomic Energy Agency (IAEA), 2021. An Introduction to Probabilistic Fault Displacement Hazard Analysis in Site Evaluation for Existing Nuclear Installations. IAEA-TECDOC-1987.

International Atomic Energy Agency (IAEA), 2022. Seismic Hazards in Site Evaluation for Nuclear Installations. Specific Safety Guide No. SSG-9 (Rev. 1).

ITHACA Working Group: ITHACA (ITaly HAzard from CApable Faulting), 2019. A Database of Active Capable Faults of the Italian Territory. Version May 2022. ISPRA Geological Survey of Italy. Web Portal. http://sgi2.isprambiente.it/ithacaweb/Mappatura.aspx.

Kerr, J., Nathan, S., Van Dissen, R., Webb, P., Brunsdon, D., King, A., . Planning for the development of land on or close to active faults, A guideline to assist resource management planners in New Zealand. http://www.mfe.govt.nz/publications/rma/planning-development-active-faults-dec04/index.html. Ministry for the Environment, Wellington, New Zealand.

Leonard, M., 2010. Earthquake fault scaling: Self-consistent relating of rupture length, width, average displacement, and moment release. Bull. Seismol. Soc. Am. 100 (5), 1971–1988. https://doi.org/10.1785/0120090189.

McCalpin, J.P., 2009. Paleoseismology, 2nd edition. Academic Press, Elsevier. International Geophysics Series 95.

Melissianos, E.M., Danciu, L., Vamvatsikos, D., Basili, R., 2023. Fault displacement hazard estimation at lifeline–fault crossings: a simplified approach for engineering applications. Bull. Earthq. Eng. 21, 4821–4849. https://doi.org/10.1007/s10518-023-01710-1.

Mildon, Z.K., Roberts, G.P., Faure Walker, J.P., Beck, J., Papanikolaou, I., Michetti, A.M., et al., 2022. Surface faulting earthquake clustering controlled by fault and shear-zone interactions. Nat. Commun. 13 (1), 7126. https://doi.org/10.1038/s41467-022-34821-5.

Ministero delle Infrastrutture e dei Trasporti, 2019. Circolare 3 luglio 2019, n. 16790. Verifiche sismiche delle grandi dighe, degli scarichi e delle opere complementari e accessorie - Istruzioni per l'applicazione della normativa tecnica (Rev. 1). Ministero delle Infrastrutture e dei Trasporti, Dipartimento per le infrastrutture, i sistemi informativi e statistici, Direzione generale per le dighe e le infrastrutture idriche ed elettriche. https://www.dighe.eu/normativa/allegati/2019_Circ_DGDighe_03-07_n_16790-Istruzioni.pdf.

Mirabella, F., Brozzetti, F., Lupattelli, A., Barchi, M.R., 2011. Tectonic evolution of a low angle extensional fault system from restored cross sections in the northern Apennines (Italy). Tectonics 30, TC6002. https://doi.org/10.1029/2011TC002890.

Moss, R.E.S., Ross, Z.E., 2011. Probabilistic fault displacement analysis for reverse faults. Bull. Seismol. Soc. Am. 101 (4), 1542–1553. https://doi.org/10.1785/0120100248.

Nemer, T.S., 2019. The Bisri dam project: a dam on the seismogenic Roum fault, Lebanon. Eng. Geol. 261, 105270. https://doi.org/10.1016/j.enggeo.2019.105270.

Nurminen, F., Boncio, P., Visini, F., Pace, B., Valentini, A., Baize, S., Scotti, O., 2020. Probability of occurrence and displacement regression of distributed surface rupturing for reverse fault. Front. Earth Sci. https://doi.org/10.3389/feart.2020.581605.

Nurminen, F., Baize, S., Boncio, P., Blumetti, A., Cinti, F., Civico, R., Guerrieri, L., 2022. New release of the worldwide database of surface ruptures for fault displacement hazard analyses, 9, p. 729. https://doi.org/10.1038/s41597-022-01835-z.

Pace, B., Visini, F., Peruzza, L., 2016. FiSH: MATLAB tools to turn fault data into seismic-Hazard models. Electron. Seismol. https://doi.org/10.1785/0220150189.

Peruzza, L., Pace, B., 2002. Sensitivity analysis for seismic source characteristics to probabilistic seismic hazard assessment in centralApennines (Abruzzo area). B. Geofis. Teor. Appl. 43, 79–100. https://doi.org/10.13053/cys-22-4-3084.

Petersen, M.D., Dawson, T.E., Chen, R., Cao, T., Wills, C.J., Schwartz, D.P., Frankel, A.D., 2011. Fault Displacement Hazard for Strike-Slip Faults. Bull. Seismol. Soc. Am. 101 (2), 805–825. https://doi.org/10.1785/0120100035.

Pezzopane, S.K., Dawson, T.E., 1996. Fault Displacement Hazard: A Summary of Issues and Information, in Seismotectonic Framework and Characterization of Faulting at Yucca Mountain, Nevada. U.S. Geological Survey Administrative Report Prepared for the U.S. Department of Energy. Chapter 9, (160 pp).

Pialli, G., Barchi, M., Minelli, G., 1998. Results of the CROP03 deep seismic reflection profile. Mem. Soc. Geol. Ital. 52, 654 (89 "Città di Castello". ISPRA–Servizio Geologico d'Italia).

Pialli, G., Plesi, G., Damiani, A.V., Brozzetti, F., 2009. Carta geologica d'Italia in scala 1: 50.000, Foglio 2.

Pucci, S., Mirabella, F., Pazzaglia, F., Barchi, M.R., Melelli, L., Tuccimei, P., Soligo, M., Saccucci, L., 2014. Interaction between regional and local tectonic forcing along a complex Quaternary extensional basin: Upper Tiber Valley, Northern Apennines, Italy. Quat. Sci. Rev. 102, 111–132. https://doi.org/10.1016/j.quascirev.2014.08.009.

Rovida, A., Locati, M., Camassi, R., Lolli, B., Gasperini, P., Antonucci, A., 2022. Catalogo Parametrico dei Terremoti Italiani (CPTI15), versione 4.0. Istituto Nazionale di Geofisica e Vulcanologia (INGV). https://doi.org/10.13127/CPTI/CPTI15.4.

Sarmiento, A., Madugo, D., Bozorgnia, Y., Shen, A., Mazzoni, S., Lavrentiadis, G., Dawson, T., Madugo, C., Kottke, A., Thompson, S., Baize, S., Milliner, C., Nurminen, F., Boncio, P., Visini, F., 2021. Fault Displacement Hazard initiative database. In: Report No. GIRS-2021-08, Revision 3.3. Los Angeles CA: The B. John Garrick Institute for the risk Sciences at UCLA Engineering. https://doi.org/10.34948/N36P48.

Sarmiento, A., Madugo, D., Shen, A., Dawson, T., Madugo, C., Thompson, S., Bozorgnia, Y., Baize, S., Boncio, P., Kottke, A., Lavrentiadis, G., Mazzoni, S., Milliner, C., Nurminen, F., Visini, F., 2024a. Database for the Fault displacement Hazard initiative project. Earthquake Spectra. https://doi.org/10.1177/87552930241262766. Epub ahead of print.

Sarmiento, A., Madugo, D., Bozorgnia, Y., Shen, A., Mazzoni, S., Lavrentiadis, G., Dawson, T., Madugo, C., Kottke, A., Thompson, S., Baize, S., Milliner, C., Nurminen, F., Boncio, P., Visini, F., 2024b. Flatfiles and Related Digital Products for the Fault Displacement Hazard Initiative Database. UCLA Dataverse, V1. Dataset. https://doi.org/10.25346/S6/Y4F9LJ.

Schlocker, J., Bonilla, M.G., 1963. Engineering geology of the proposed nuclear power plant site on bodega head, sonoma county, California. In: Report TEI-844, US Department of the Interior. Geological Survey. Washington DC.

SM Working Group, 2015. Guidelines for Seismic Microzonation, Conference of Regions and Autonomous Provinces of Italy – Civil Protection. Department, Rome. https://www.centromicrozonazionesismica.it/documents/18/GuidelinesForSeismicMicrozonation.pdf.

Takao, M., Tsuchiyama, J., Masashi, A., Testushi, K., 2013. Application of probabilistic fault displacement hazard analysis in Japan. Jpn. Assoc. Earthquake Eng. 13 (1), 17–36. https://doi.org/10.5610/jaee.13.17U.S.

Testa, A., Valentini, A., Boncio, P., Pace, B., Visini, F., Mirabella, F., Pauselli, C., 2021. Probabilistic fault displacement hazard analysis of the Anghiari - Città di Castello normal fault (Italy). Ital. J. Geosci. 140 (3), 327–346, 13 figs., 1 tab. https://doi.org/10.3301/IJG.2021.07.

Technical Commission on Seismic Microzonation, 2015. Land Use Guidelines for Areas with Active and Capable Faults (ACF), Conference of the Italian Regions and Autonomous Provinces – Civil Protection Department, Rome. https://www.centromicrozonazionesismica.it/documents/23/FAC_ing.pdf.

Testa, A., Boncio, P., Baize, S., Mirabella, F., Pucci, S., Pace, B., Riesner, M., Pauselli, C., Ercoli, M., Benedetti, L., Di Chiara, A., Civico, R., 2023. Paleoseismological Constraints of the Anghiari Fault in the Altotiberina Low-Angle Normal Fault System (Northern Apennines, Italy). https://doi.org/10.22541/essoar.169111453.36853267/v1.

Valentini, A., Fukushima, Y., Contri, P., Ono, M., Sakai, T., Thompson, S., Viallet, E., Annaka, T., Chen, R., Moss, R., Petersen, M., Visini, F., Youngs, R., 2021. Probabilistic fault displacement hazard assessment for nuclear installations according to iaea safety standards. Bull. Seismol. Soc. Am. 111, 2661–2672.

Wells, D.L., Coppersmith, K.J., 1993. Likelihood of surface rupture as a function of magnitude. Seismol. Res. Seismol. Res. Lett. 64 (1), 54.

Wells, D.L., Coppersmith, K.J., 1994. New empirical relationships among magnitude, rupture length, rupture width, rupture area, and surface displacement. Bull. Seismol. Soc. Am. 84, 974–1002. https://doi.org/10.1785/0120210083.

Yang, S., Mavroeidis, G.P., 2018. Bridges crossing fault rupture zones: a review. Soil Dyn. Earthq. Eng. 113, 545–571. https://doi.org/10.1016/j.soildyn.2018.03.027.

Youngs, R.R., Arabasz, W.J., Anderson, R.E., Ramelli, A.R., Ake, J.P., Slemmons, D.B., Mccalpin, J.P., Doser, D.I., Fridrich, C.J., Swan, F.H. Iii, Rogers, A.M., Yount, J.C., Anderson, L.W., Smith, K.D., Bruhn, R.L., Knuepfer, L.K., Smith, R.B., Depolo, C.M., O'leary, K.W., Coppersmith, K.J., Pezzopane, S.K., Schwartz, D.P., Whitney, J.W., Olig, S.S., Toro, G.R., 2003. A methodology for probabilistic fault displacement hazard analysis (PFDHA). Earthquake Spectra 19 (1), 191–219. https://doi.org/10.1193/1.1542891.

Zhang, Y.S., Shi, J.S., Sun, P., Yang, W.M., Yao, X., Zhang, C.S., Xiong, T.Y., 2013. Surface ruptures induced by the Wenchuan earthquake: their influence widths and safety distances for construction sites. Eng. Geol. 166, 245–254. https://doi.org/10.1016/j.enggeo.2013.09.010.